Environ Geochem Health (2023) 45:3971–3983
https://doi.org/10.1007/s10653-023-01479-x

ORIGINAL PAPER

Degradation behaviors and accumulative effects of coexisting chlorobenzene congeners on the dechlorination of hexachlorobenzene in soil by nanoscale zero-valent iron

Qi Wang

Received: 4 November 2022 / Accepted: 4 January 2023 / Published online: 11 January 2023

Abstract It is well known that many chlorinated organic pollutants can be dechlorinated by nanoscale zero-valent iron. However, in the real chlorinated organic compounds contaminated soil, the congeners of high- and low-chlorinated isomer often coexist and their dechlorination behaviors are poorly known, such as hexachlorobenzene (HCB). In this work, the degradation behaviors of three coexisting chlorobenzene congeners pentachlorobenzene (PeCB), 1,2,4,5-tetrachlorobenzene (1,2,4,5-TeCB) and 1,2,4-trichlorobenzene (1,2,4-TCB) and the influence of initial pH and reaction temperature on the dechlorination of HCB in HCB-contaminated soil by nanoscale zero-valent iron were studied. The amount and extent of accumulated coexisting chlorobenzenes was analyzed under different environmental conditions. The results indicate that nanoscale zero-valent iron can improve the degradation efficiency of highly toxic chlorinated benzenes and reduce the accumulative effects of highly toxic chlorinated benzenes on dechlorination of HCB. The accumulative effects of three coexisting chlorobenzene congeners on the dechlorination of HCB were ranked as follows: 1,2,4-TCB > 1,2,4,5-TeCB > PeCB.

Q. Wang (✉)
Beijing Key Laboratory for Risk Modeling and Remediation of Contaminated Sites, National Engineering Research Center of Urban Environmental Pollution Control, Beijing Municipal Research Institute of Eco-Environmental Protection, Beijing 100037, China
e-mail: wq020704@126.com

Keywords Hexachlorobenzene · Accumulative effect · Coexisting chlorobenzene congener · Nanoscale zero-valent iron · Dechlorination

Introduction

Since HCB was first introduced in 1933 (Barber et al. 2005), the compound was used in pyrotechnic compositions for military purposes, and as porosity controller in the manufacture of electrodes, and in chemical industries, and also as a selective fungicide for seed treatment in agriculture (Starek-Swiechowicz et al. 2017). HCB is classified as one of the 12 persistent organic pollutants controlled in the first phase by United Nations Stockholm Convention and poses adverse effects on human health and environment (Dhaibar et al. 2021; Drysdale et al. 2021; Umulisa et al. 2020). Although the commercial production of HCB has been prohibited for decades all over the world, it is still produced as an industrial by-product during synthesis of some chlorinated organic solvents and pesticides (Bailey, 2001; Jiang et al. 2018a).

HCB and low-chlorinated benzenes have been found in various matrixes, such as air, soil, water (Brahushi et al. 2017), wastewater (Yuan et al. 2020), sediment (Gao et al. 2015), vegetation and breast milk with concentration levels of approximately 105 ppm (Wang et al. 2010; Zhou et al. 2013). The concentration of HCB in soil was 8.01 ng/g in Anhui, China (Song et al. 2017; Wang

et al. 2010). Generally, soil was known to perform as the final acceptor (Liu et al. 2015) for the majority mass of HCB, because that HCB in the troposphere can be removed from the gas phase via atmospheric deposition to water and soil, as well as its lower octanol/water partition coefficients, soil/air partition coefficients (Meijer et al. 2003) and adsorption capacity on particulate matter. So, HCB pollution in soil poses a serious challenge around the world, including the USA, Germany, Australia, Japan, Brazil (Jiang et al. 2018b) and China. The removal of HCB from soil is of great concern and attracts considerable scientific and regulatory interests, due to the high toxicity, great bioaccumulation and persistence of HCB in the environment.

In the past several years, a number of studies have been carried out to explore the treatment operations for removal of HCB, such as electrokinetic remediation (Oonnittan et al. 2008, 2009; Yuan et al. 2006a), microwave remediation (Yuan et al. 2006b), base-catalyzed dechlorination (Huang et al. 2014), ozone-based processes (Derco et al. 2015), photo-catalytic degradation (Pan et al. 2020), microbial aerobic mineralization (Matheus et al. 2000; Takagi et al. 2009) and microbial anaerobic degradation (Jiang et al. 2015; Liu et al. 2010a, 2010b; Yan et al. 2015). Although anaerobic degradation is believed to be a competitive and efficient method for decomposing HCB for the past few years and HCB can be dechlorinated to low-toxic chlorinated benzenes under the anaerobic condition by inducing the native microbial activity (Chen et al. 2010; Wu et al. 2002), anaerobic microorganisms and desirable degradation time are hard to acquire. It has been proved that zero-valent iron could increase the efficiency of HCB degradation and could be used for remediation of HCB-contaminated sites (Chen et al. 2014; Garbou et al. 2019; Shih et al. 2009, 2011; Su et al. 2012; Wan et al. 2010; Zhu et al. 2010). However, in the real HCB-contaminated soil, there are a lot of chlorobenzene congeners, such as PeCB, 1,2,4,5-TeCB and 1,2,4-TCB, coexisting with HCB and the effect on the degradation capacity of HCB is poorly known.

This work aims to investigate the degradation behaviors of three coexisting chlorobenzene congeners PeCB, 1,2,4,5-TeCB and 1,2,4-TCB and their accumulative effects on the reductive dechlorination of HCB by nanoscale zero-valent iron in HCB-contaminated soil under different environmentally relevant conditions such as initial pH and reaction temperatures.

Materials and methods

Soil materials and chemicals

Real HCB-contaminated soil was sampled from a site, producing certain chlorinated organic solvent, located in Beijing, China, where HCB was used as intermediate for more than 30 years. The soil was dried, ground and sieved with a 2 mm sieve to remove debris, then stored in the dark at 4 °C. In all soil samples, the initial concentrations of HCB, PeCB, 1,2,4,5-TeCB and 1,2,4-TCB were quantified in the range of 2.00–2.80 mg/g d w soil, 0.10–0.35 mg/g d w soil, 0.14–0.49 mg/g d w soil and 0.25–0.90 mg/g d w soil, separately. The pH of soil measured is 7.6 by the mixing of soil and water (1:1, w/w).

The nanoscale zero-valent iron was provided by Guangzhou Hongwu New Material Technology Co., China., with the average particle sizes of 102.4 ± 20.8 nm. Acetic acid was selected as a nutriment. NaOH and H_2SO_4 were used to adjust pH of the reaction system. Na_2SO_4 was oven-dried at 400°C for 4 h before use. Dichloromethane and acetone were used for the extraction of HCB. All the reagents mentioned above were analytical grade. Each vial including 15 mL HCB sample was mixed with 0.1 g of nanoscale ZVI particles.

Batch dechlorination experiments

The 200 g treated real HCB-contaminated soil sample was added to the jar and mixed with a certain proportion of deionized water to form slurry. 0.8 g acetic acid and 0.2 g iron nanoparticles were added, respectively. Then, the pH of slurry was adjusted using NaOH and H_2SO_4 solution and the initial pH was measured with a pH meter (PHSJ-4A, Shanghai ShengCi Instrument Company, China). The bottle was sealed, with N_2 gas sparged, and was incubated under the set temperature in the biochemical incubator for 23 days. At the end of each experiment, the supernatant of the mixture was separated from the solid residue using suction filter device. The quantification and structural confirmation of all four chlorobenzenes in the mud phase were analyzed using gas chromatograph–mass spectrometer

(Thermo Fisher ITQ 1100). Each experiment was conducted in triplicate. The structure and surface morphology of nanoscale zero-valent iron was characterized using a Hitachi S-4800 Field Emission Scanning Electron Microscope (SEM).

Separation and analysis of chlorinated aromatic compounds

20 g mud sample was mixed with 20 g anhydrous Na_2SO_4 thoroughly, in order to remove the moisture. The HCB in dried mud sample was extracted with 100 mL dichloromethane/acetone (1:1, v/v) by 2 h ultra-sonication. After the sample was filtered and cleaned repeatedly with dichloromethane, the supernatant was concentrated to about 2 ml in a parallel vacuum evaporator. Then, the evaporated sample was further concentrated to below 1 ml by a nitrogen stream and finally was diluted to 1 ml with dichloromethane for analysis.

The gas chromatograph was equipped with a HP-5 capillary column (30 m length × 0.32 mm inside diameter × 0.25 μm film thickness). The temperature program of the GC started at 40 °C and was held for 4 min. Then, the column was sequentially heated to 160 °C at rate 10 °C/min (1 min), 280 °C at rate 10 °C/min (4 min), 300 °C at rate 10 °C/min (5 min). The flow rate of carrier gas (nitrogen 99.999%) was 1.5 mL/min. The inlet temperature was 270 °C and the injection volume of extract was 1.00 μL in a splitless mode.

The mass spectrometer was equipped with an electron ionization (EI) source and operation conditions were ion source temperature 275 °C, quadropole temperature 150 °C and mass scan range 35–500 amu.

Chlorobenzenes were identified by comparing their varied retention times corresponding to reference substances. All the analyses were conducted in duplicate soil samples. The result of internal standard recovery experiment showed that the average recoveries of HCB, PeCB, 1,2,4,5-TeCB and 1,2,4-TCB were, respectively, 104.1%, 103.9%,102.4% and 101.1%.

Results and discussion

SEM characterization

Figure 1 shows the structure and surface morphology of nanoscale zero-valent iron. SEM micrographs reveal that nanoparticles are spherical, with a chain structure, probably because of the static magnetism and surface force between small particles, and the agglomeration phenomenon is also seen in the image. The chain structure can increase the adsorption space and then improve reduction effectiveness.

Degradation behaviors of HCB and coexisting chlorobenzene congeners under different initial pH

Figure 2 is plot of residual concentrations of HCB and three coexisting chlorobenzene congeners versus reaction time under different initial pH. As shown in Fig. 2a, the residual concentrations of HCB decreased with the increase in initial pH. The lower residual concentrations of HCB were found under acidic conditions (pH = 3) and slightly acidic conditions (pH = 5), whereas higher residual concentrations were found under alkaline conditions (pH = 9 and pH = 11), within the initial pH range of 3.0–11.0. These indicate that the higher degradation rate of HCB can be obtained under acidic and slightly acidic reaction system and the degradation rate of HCB is lower under alkaline reaction system. The lower degradation rate of HCB under alkaline reaction system could be attributed to the feedback inhibition caused by accumulation of low-toxic chlorinated benzenes. In the process of degradation, degradation activity of substrate can be inhibited because of decline of enzyme activity, resulting from accumulation of intermediate metabolite (Zhou, 2002).

The degradation activity of three coexisting chlorobenzene congeners in real HCB-contaminated soil

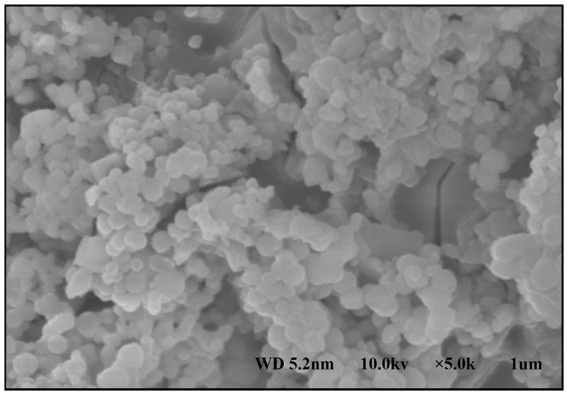

Fig. 1 SEM image of nanoscale zero-valent iron

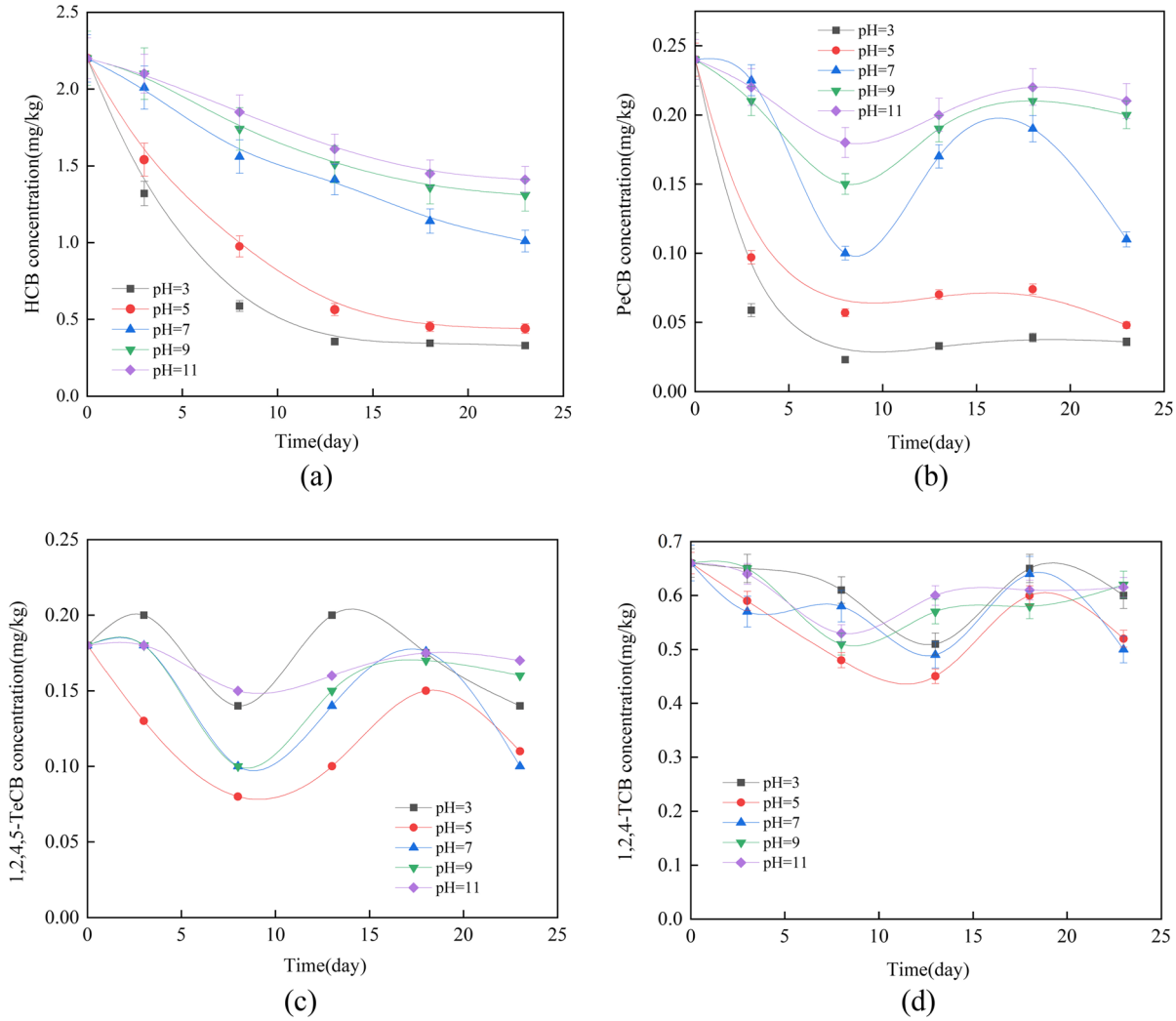

Fig. 2 Concentration versus time in real HCB-contaminated soil sample under different initial pH

was investigated with the initial pH in the range of 3.0–11.0. As depicted in Fig. 2b, the residual concentrations of PeCB decreased rapidly, within reaction time of 23 days, and then increased slowly, following with decreasing under all initial pH condition, which is lower under acidic conditions and slightly acidic conditions. The same results are also observed for 1,2,4,5-TeCB and 1,2,4-TCB. The dechlorination of HCB followed usually a stepwise pathway:

$$\begin{aligned}\mathrm{HCB} \rightarrow\ & \mathrm{PeCB} \rightarrow 1,2,4,5\text{ - TeCB}/1,2,3,4\text{ - TeCB} \\ & \rightarrow \mathrm{Trichlorobenzene} \rightarrow \mathrm{Dichlorobenzene} \\ & \rightarrow \mathrm{Monochlorobenzene}\end{aligned}$$

HCB → PeCB → 1,2,4,5-TeCB/1,2,3,4-TeCB → Trichlorobenzene → Dichlorobenzene → Monochlorobenzene(Chen et al. 2014; Deng et al. 2017). Thus, the reason for the discontinuous decreasing and the different degradation behaviors of three chlorobenzenes is that there is accumulation of three kind of dichlorobenzene intermediates, depending on reaction rate under different initial pH, existed in the process of degradation by nanoscale zero-valent iron.

The reaction rate equation and pseudo-first-order model were applied to describe the dechlorination of HCB as follows:

Reaction rate equation : $\nu = -\mathrm{d}C/\mathrm{d}t$ where ν is reaction rate per unit biomass, C is time-dependent concentration of HCB, C_0 is the initial concentration of HCB, k is the pseudo-first-order rate constant (d^{-1}) and t is the reaction time. A nonlinear regression procedure was based on the Marquardt–Levenberg algorithm and the goodness of correlation was evaluated with the correlation coefficient.

Figure 3 shows the reaction rate of four coexisting chlorobenzene congeners HCB, PeCB, 1,2,4,5-TeCB and 1,2,4-TCB under different initial pH. As shown, the reaction rate of three coexisting chlorobenzene congeners had a "V" type change. For PeCB, 1,2,4,5-TeCB and 1,2,4-TCB, the calculated value of reaction rate may not be "positive" or "negative" invariably, because that the production and degradation of three coexisting chlorobenzene congeners proceed simultaneously (Jiang et al. 2015). So, when the calculated value of ν is positive, the degradation of low-toxic chlorinated benzenes is predominant and the concentrations of chlorobenzenes decrease constantly, that is, there is no accumulation in the degradation. Otherwise, when the calculated value of ν is negative, the production of low-toxic chlorinated benzenes is predominant and the concentrations of chlorobenzenes increase constantly and there is accumulation. It is evident that the reaction rate of HCB is higher than other three coexisting chlorobenzene congeners, especially in the acidic (pH = 3) and slightly acidic conditions (pH = 5), and PeCB comes second.

For every single curve, the figure area under the "0" calibration can be calculated with the method of calculus and results are shown in Table 1. The size of the area reflects the amount and extent of accumulated coexisting chlorobenzenes. It is also evident that the accumulative amount and the extent of 1,2,4-TCB are the most in the acidic and alkaline condition, especially, acidic conditions (pH = 3) and slightly acidic conditions (pH = 5). The results indicate that the degradation reaction rate of congeners of high-chlorinated isomer is higher in the acidic condition during the degradation process with nanoscale zero-valent iron. The reason is that the dissolution of the passivating hydroxide layer on nanoscale zero-valent iron was facilitated at low pH, which increased the reactivity, and at higher pH, ferrous and ferric hydroxides were formed, which could have resulted in hydroxide covering the Fe^0 surfaces and hampering the electron transfer (Chen et al. 2014). It has been proved that HCB can be dechlorinated to low-toxic chlorinated benzenes under the anaerobic condition by inducing the native microbial activity, which followed the dechlorination pathway (Brahushi et al. 2004; Chen et al. 2010) described above. So, the degradation of HCB by nanoscale zero-valent iron is predominant under acidic condition, and the role of native microbial is predominant under alkaline condition when the dechlorination of nanoscale zero-valent iron is weakened.

In Fig. 4, the degradations of HCB under different initial pH ran well with the pseudo-first-order model, which can be observed from the R^2 coefficients in Table 2. The results of data correlation and fitting parameters are reported in Table 2. Pseudo-first-order reaction rate constants were estimated for dechlorination of HCB by nanoscale zero-valent iron particles in different initial pH ranging from 0.2685 d^{-1} at pH3 to 0.0211 d^{-1} at pH11. The rate constant increases with initial pH decrease, which is in accord with that reported by Shih et al. In addition, rate constants under acidic and slightly acidic conditions were one order of magnitude higher than alkaline condition. It is proved again that the dechlorination of HCB by nanoscale zero-valent iron is favorable under acidic and slightly acidic reaction system.

Degradation behaviors of HCB and coexisting chlorobenzene congeners under different reaction temperature

Figure 5 is plot of residual concentrations of HCB and three coexisting chlorobenzene congeners versus reaction time under different reaction temperature.

It is obvious that the residual concentrations of HCB decrease with increasing reaction temperature, within a temperature range of 15−55 °C. When the reaction temperature was up to 45 °C, the residual concentration of HCB was almost the lowest during the degradation of 23 days. This implies that the degradation rate of HCB was almost the highest with a reaction temperature of 45°C. Similarly, it can be concluded that the lower degradation rate of HCB in room temperature is due to accumulation of the large amount of 1,2,4-TCB, according to the degradation behaviors of coexisting chlorobenzene congeners under different reaction temperatures. It is observed from Fig. 5 that the concentrations had a "wave" type change within a temperature range of 15 − 55 °C for

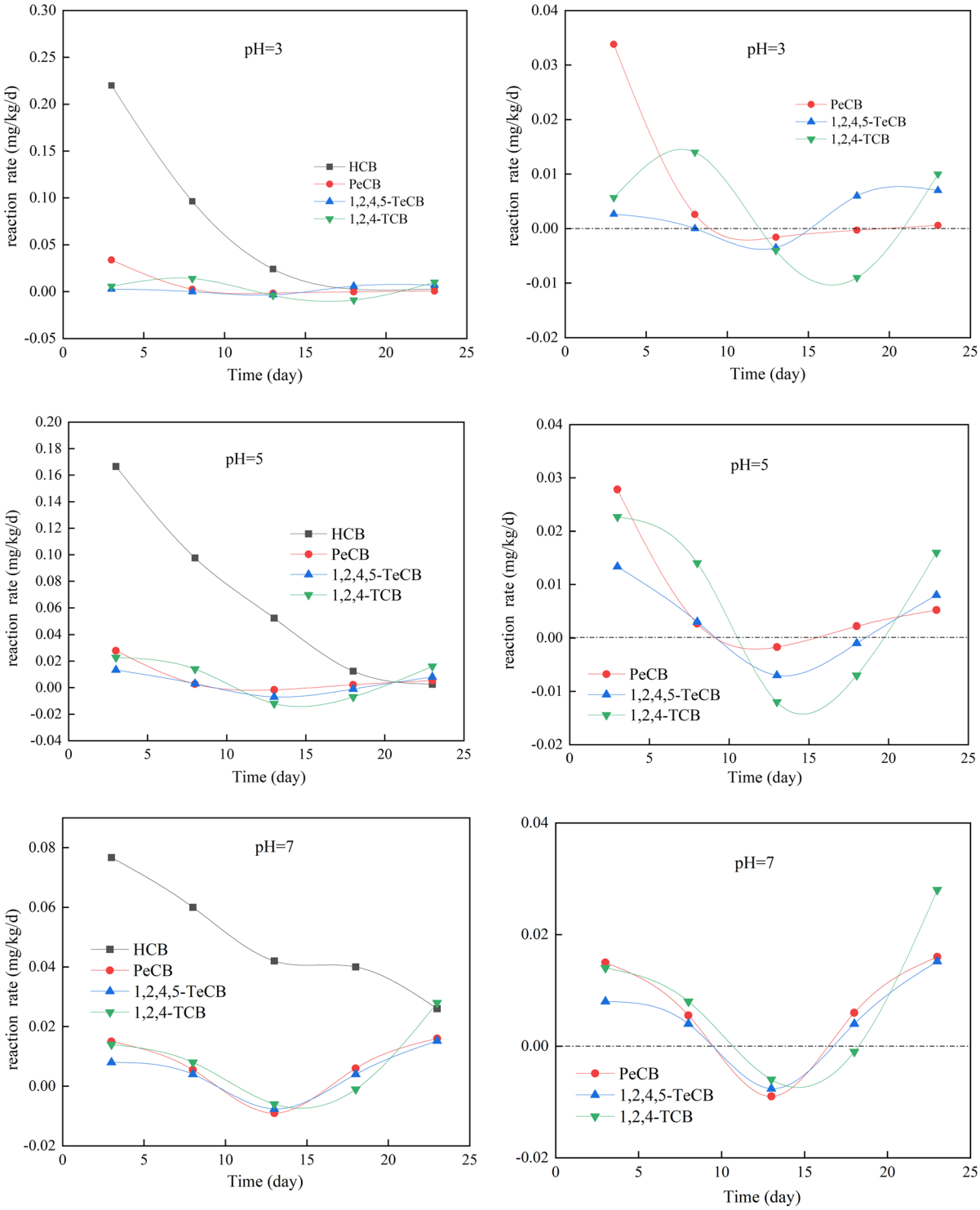

Fig. 3 The reaction rate of HCB and three coexisting chlorobenzene congeners under different initial pH

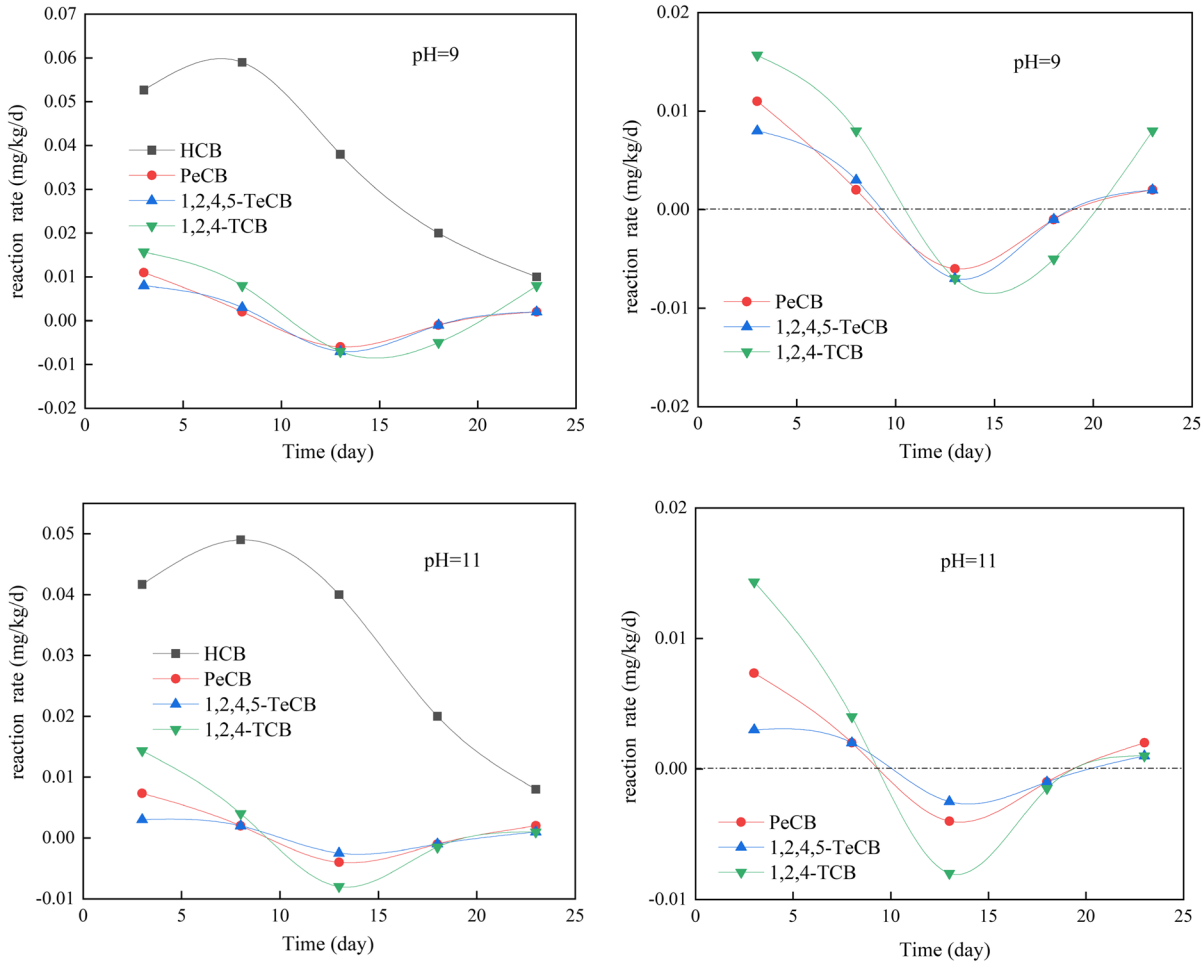

Fig. 3 (continued)

Table 1 The accumulation of three coexisting chlorobenzene congeners (mg/kg)

	pH = 3	pH = 5	pH = 7	pH = 9	pH = 11
PeCB	0.0083	0.0054	0.03136	0.04963	0.0205
1,2,4,5-TeCB	0.0122	0.0336	0.02761	0.05063	0.0135
1,2,4-TCB	0.0473	0.0682	0.02458	0.05223	0.0396

two coexisting chlorobenzene congeners 1,2,4,5-TeCB and 1,2,4-TCB. The residual concentrations were almost the lowest when the reaction temperature is 45 °C, comparing with other reaction temperature. The reason of increasing reaction temperature could facilitate the degradation of HCB is that higher temperature is helpful to the desorption of organic

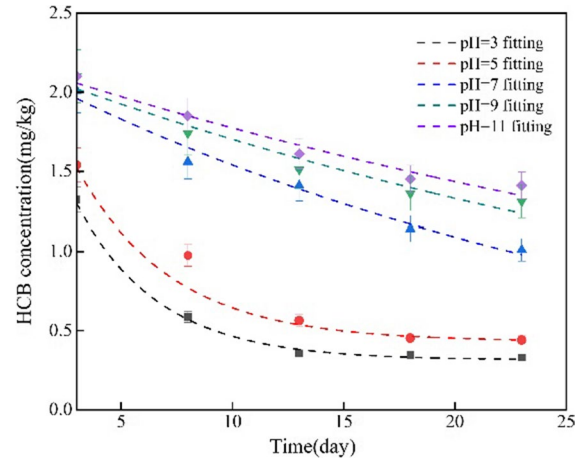

Fig. 4 The nonlinear regression fit of the HCB data to the pseudo-first-order model under different initial pH

Table 2 Rate constants of HCB by nanoscale zero-valent iron under different initial pH

Initial pH	Rate constant(k)	correlation coefficient (R^2)
3	0.2685	0.973
5	0.2336	0.964
7	0.0340	0.983
9	0.0243	0.952
11	0.0211	0.965

pollutants from soil (Jiang et al. 2018a) and sterilize the microbes that influence decomposition of pollutants in the soil (Liu et al. 2014).

The plots of the reaction rate of three coexisting chlorobenzene congeners under different reaction temperature are presented in Fig. 6. It can be observed that the reaction rate of three coexisting chlorobenzene congeners had a "V" type change similarly and indicate that the accumulation exists in the process of degradation within reaction temperature ranging from 15 to 55 °C. The accumulation period of 1,2,4-TCB was longer, compared with the that of PeCB and 1,2,4,5-TeCB. Additionally, the size of the area calculated and shown in Table 3 reflects that the amount of 1,2,4-TCB is more than the other two chlorobenzenes under any reaction temperature.

A plot (Fig. 7) of HCB degradations under different reaction temperature shew good correlation similarly. It is observed in Table 4 that

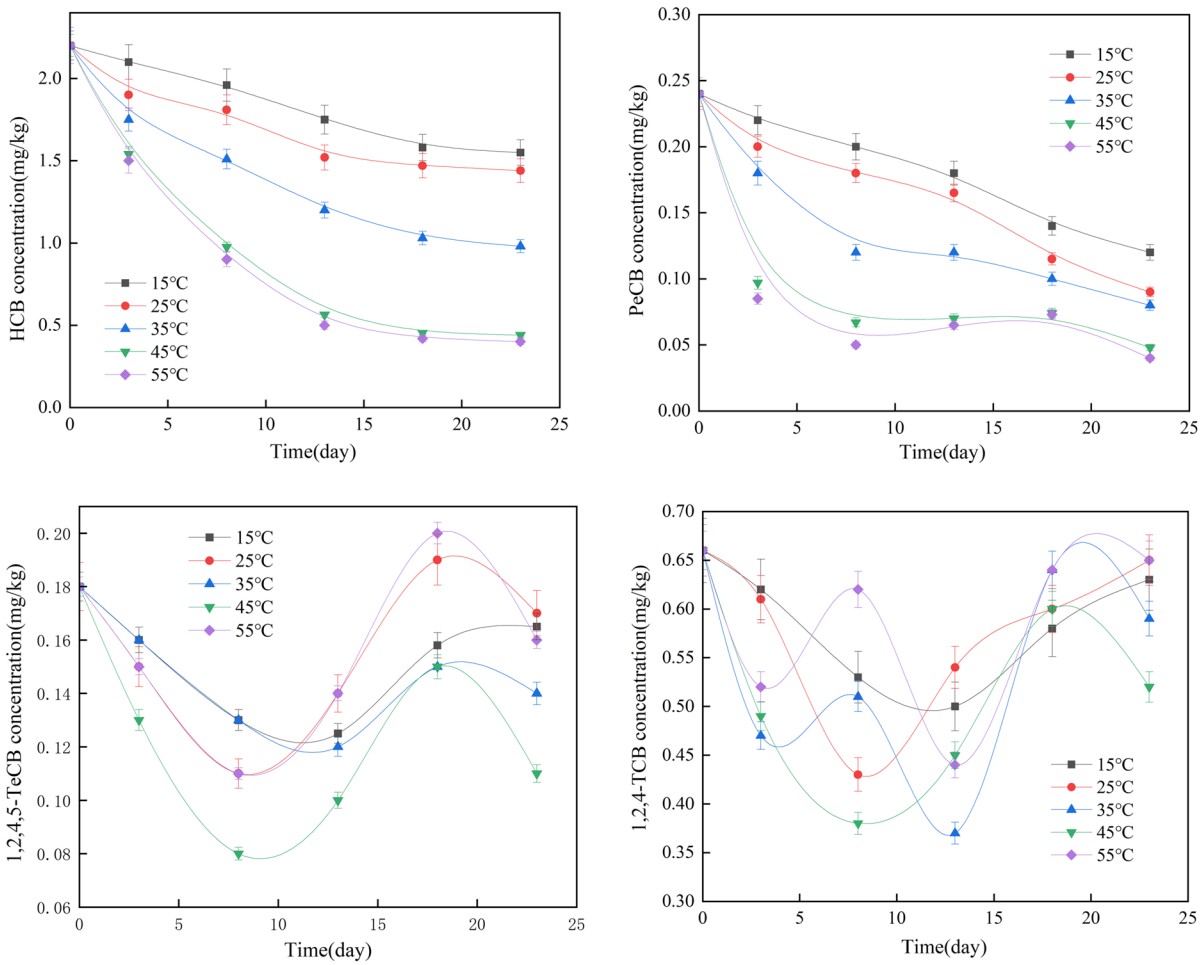

Fig. 5 Concentration versus time in real HCB-contaminated soil sample under different reaction temperature

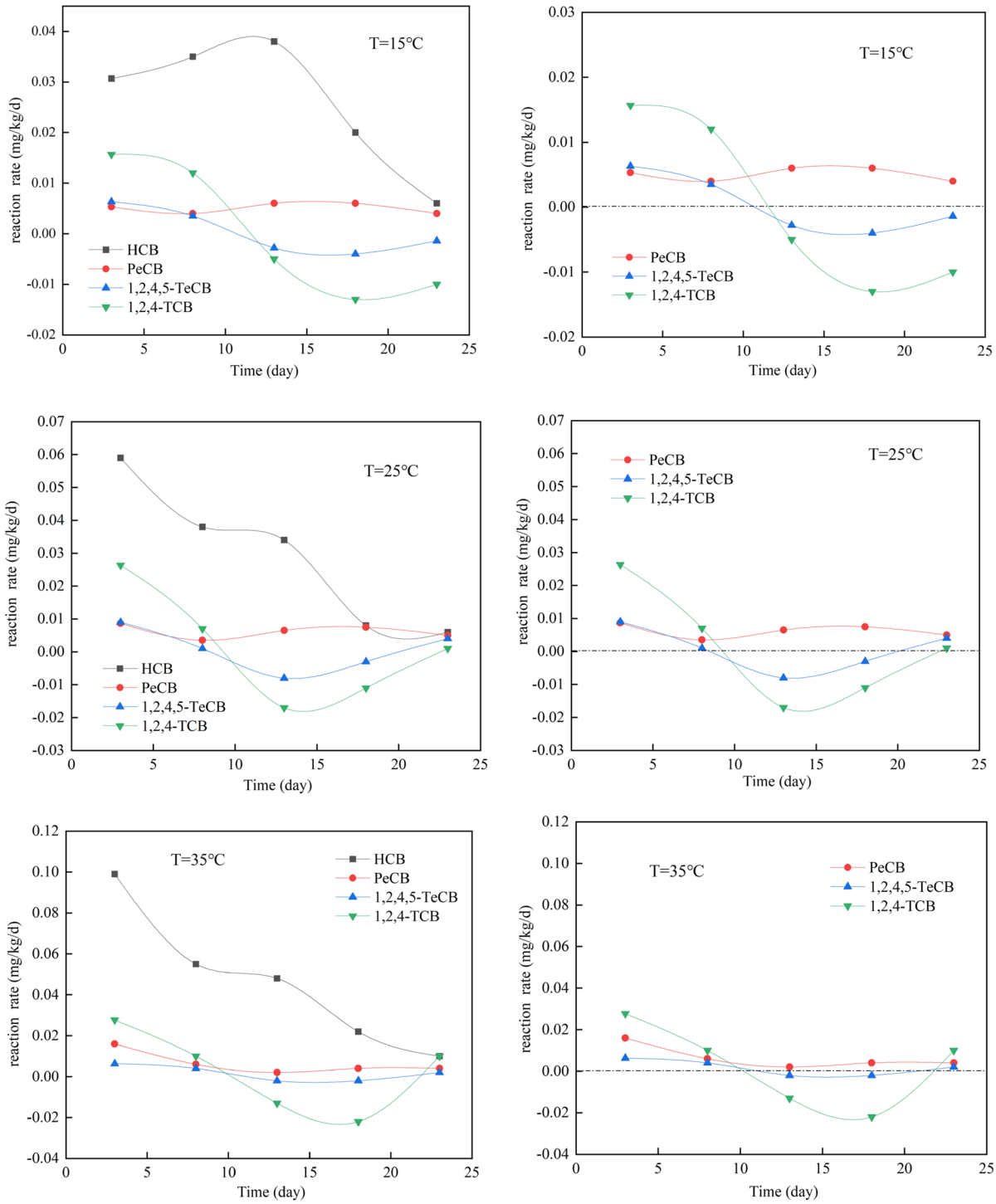

Fig. 6 The reaction rate of HCB and three coexisting chlorobenzene congeners under different reaction temperature

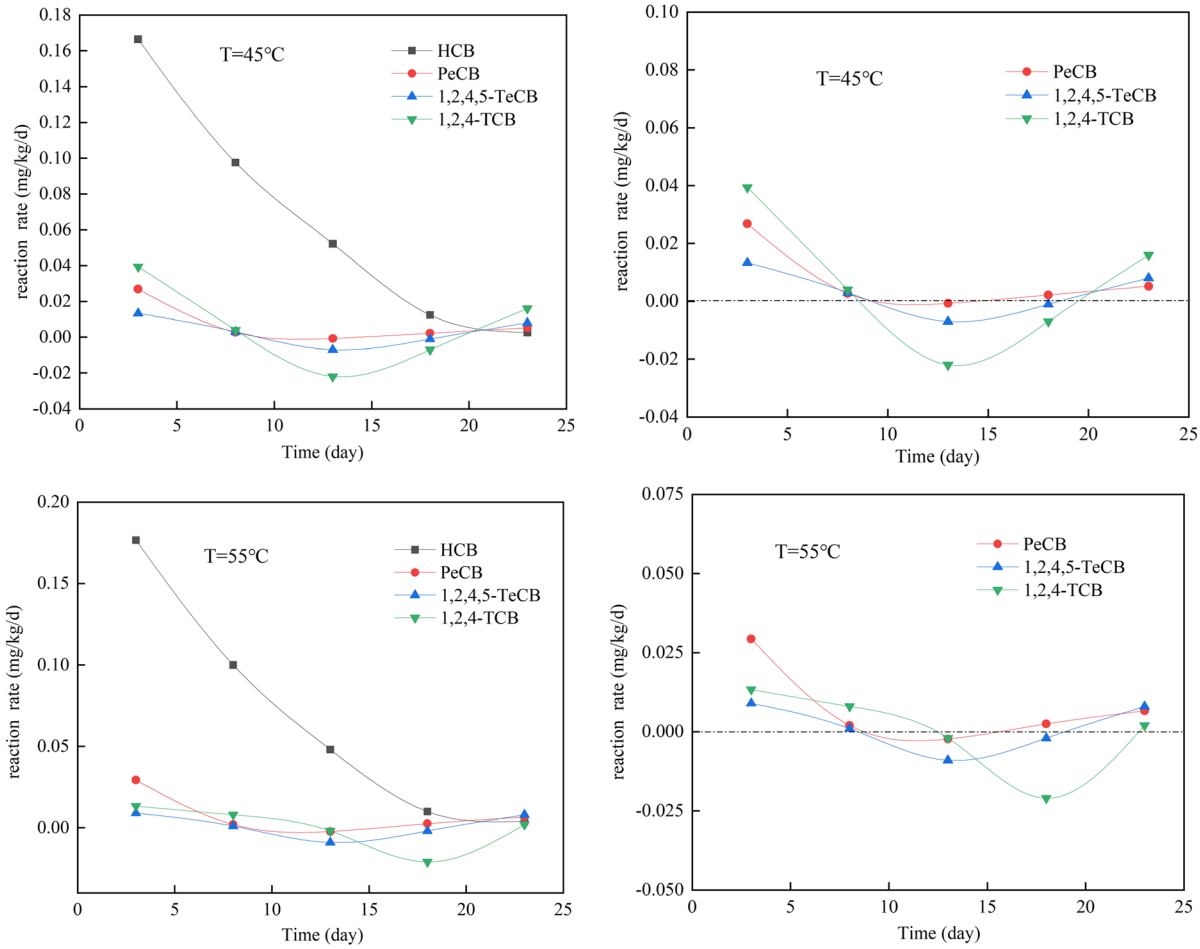

Fig. 6 (continued)

Table 3 The accumulation of three coexisting chlorobenzene congeners (mg/kg)

	15 °C	25 °C	35 °C	45 °C	55 °C
PeCB	–	–	–	0.0019	0.0077
1,2,4,5-TeCB	–	0.0496	0.0146	0.0339	0.0486
1,2,4-TCB	–	0.1280	0.1471	0.1274	0.1070

pseudo-first-order reaction rate constants ranged from 0.0166 d^{-1} at 15 °C to 0.1920 d^{-1} at 15 °C. The rate constants under higher reaction temperature were one order of magnitude higher than lower reaction temperature. These reveal that 45–55 °C are more favorable for fast degradation of HCB.

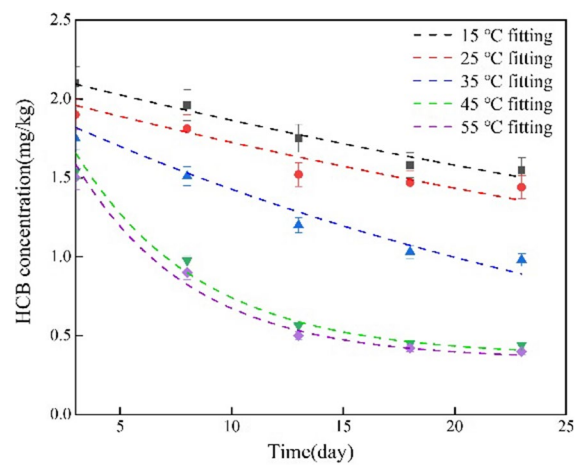

Fig. 7 The nonlinear regression fit of the HCB data to the pseudo-first-order model under different reaction temperature

Table 4 Rate constants of HCB by nanoscale zero-valent iron under different reaction temperature

Reaction temperature(°C)	Rate constant(k)	Standard error(R^2)
15	0.0166	0.970
25	0.0170	0.896
35	0.0311	0.930
45	0.1786	0.953
55	0.1920	0.960

Conclusions

This study investigated the degradation behaviors of coexisting chlorobenzene congeners and the influence of them on the dechlorination of HCB in HCB-contaminated soil by nanoscale zero-valent iron under different environmental conditions. Parameters that may affect the degradation behaviors of coexisting chlorobenzene congeners and HCB, such as initial pH and reaction temperature, were studied. From this study the following conclusions can be drawn: (1) there exist accumulations of coexisting chlorobenzene congeners in the degradation and the accumulated amount and extent vary with environmentally relevant conditions. (2) degradation activity of HCB was reduced due to the feedback inhibition caused by accumulation of coexisting chlorobenzene congeners and the feedback inhibition varies from environmental conditions. (3) 1,2,4-TCB exhibited the strongest inhibitive effect under different initial pH and reaction temperature.

Acknowledgements This work was supported by Foundation of Beijing Municipal Research Institute of Eco-Environmental Protection (Y2017-102).

Author contributions Qi Wang wrote the main manuscript text and prepared figures.

Funding Foundation of Beijing Municipal Research Institute of Eco-Environmental Protection, Y2017-102.

Declarations

Conflict of interest There are no conflicts of interest to declare.

References

Bailey, R. E. (2001). Global hexachlorobenzene emissions. *Chemosphere, 43*(2), 167–182.

Barber, J. L., Sweetman, A. J., Van Wijk, D., & Jones, K. C. (2005). Hexachlorobenzene in the global environment: Emissions, levels, distribution, trends and processes. *Science of the Total Environment, 349*(1–3), 1–44.

Brahushi, F., Dorfler, U., Schroll, R., & Munch, J. C. (2004). Stimulation of reductive dechlorination of hexachlorobenzene in soil by inducing the native microbial activity. *Chemosphere, 55*(11), 1477–1484.

Brahushi, F., Kengara, F. O., Song, Y., Jiang, X., Munch, J. C., & Wang, F. (2017). Fate Processes of chlorobenzenes in soil and potential remediation strategies: A review. *Pedosphere, 27*(3), 407–420.

Chen, I. M., Wanitchapichat, W., Jirakittayakorn, T., Sanohniti, S., Sudjarid, W., Wantawin, C., Voranisarakul, J., & Anotai, J. (2010). Hexachlorobenzene dechlorination by indigenous sediment microorganisms. *Journal of Hazardous Materials, 177*(1–3), 244–250.

Chen, W. F., Pan, L., Chen, L. F., Wang, Q., & Yan, C. C. (2014). Dechlorination of hexachlorobenzene by nano zero-valent iron/activated carbon composite: Iron loading, kinetics and pathway. *RSC Advances, 4*, 46689.

Deng, S., Kang, S., Feng, N., Zhu, J., Yu, B., Xie, X., & Chen, J. (2017). Mechanochemical mechanism of rapid dechlorination of hexachlorobenzene. *Journal of Hazardous Materials, 333*, 116–127.

Derco, J., Dudas, J., Valickova, M., Simovicova, K., & Kecskes, J. (2015). Removal of micropollutants by ozone-based processes. *Chemical Engineering and Processing, 94*, 78–84.

Dhaibar, H. A., Patadia, H., Mansuri, T., Shah, R., Khatri, L., Makwana, H., Master, S., & Robin, P. (2021). Hexachlorobenzene, a pollutant in hypothyroidism and reproductive aberrations: A perceptive transgenerational study. *Environmental Science and Pollution Research International, 28*(9), 11077–11089.

Drysdale, M., Ratelle, M., Skinner, K., Garcia-Barrios, J., Gamberg, M., Williams, M., Majowicz, S., Bouchard, M., Stark, K., Chalil, D., & Laird, B. D. (2021). Human biomonitoring results of contaminant and nutrient biomarkers in Old Crow, Yukon Canada. *Science of the Total Environment, 760*, 143339.

Gao, L. R., Xia, D., Tian, H. Z., Zhang, H. J., Liu, L. D., & Wang, Y. W. (2015). Concentrations and distributions of 18 organochlorine pesticides listed in the Stockholm convention in surface sediments from the Liaohe river basin China. *Journal of Environmental Science Health B, 50*(5), 322–330.

Garbou, A. M., Liu, M., Zou, S., & Yestrebsky, C. L. (2019). Degradation kinetics of hexachlorobenzene over zero-valent magnesium/graphite in protic solvent system and modeling of degradation pathways using density functional theory. *Chemosphere, 222*, 195–204.

Huang, H., Jiang, J. G., Xiao, Y., Chen, X. J., & Liu, S. (2014). A novel and efficient method for dechlorination of hexachlorobenzene using a sodium carbonate/glycerol system. *Chemical Engineering Journal, 256*, 205–214.

Jiang, D., Zeng, G., Huang, D., Chen, M., Zhang, C., Huang, C., & Wan, J. (2018a). Remediation of contaminated soils by enhanced nanoscale zero valent iron. *Environmental Research, 163*, 217–227.

Jiang, L., Wang, Q., Liu, H., & Yao, J. J. (2015). Influence of degradation behavior of coexisting chlorobenzene congener pentachlorobenzene, 1,2,4,5-tetrachlorobenzene and 1,2,4-trichlorobenzene on the anaerobic reductive dechlorination of hexachlorobenzene in dye-plant contaminated soil. *Water Air & Soil Pullution, 226*(9), 1–9.

Jiang, Y., Shang, Y., Yu, S., & Liu, J. (2018b). Dechlorination of hexachlorobenzene in contaminated soils using a nanometallic Al/CaO dispersion mixture: Optimization through response surface methodology. *Internatrional Journal Environment Research and Public Health, 15*(5), 852.

Liu, C., Jiang, X., Wang, F., Yang, X., & Wang, T. (2010a). Hexachlorobenzene dechlorination as affected by nitrogen application in acidic paddy soil. *Journal of Hazardous Materials, 179*(1–3), 709–714.

Liu, C. Y., Jiang, X., Yang, X. L., & Song, Y. (2010b). Hexachlorobenzene dechlorination as affected by organic fertilizer and urea applications in two rice planted paddy soils in a pot experiment. *Science of the Total Environment, 408*(4), 958–964.

Liu, C., Xu, X., & Fan, J. (2015). Accelerated anaerobic dechlorination of DDT in slurry with hydragric acrisols using citric acid and anthraquinone-2,6-disulfonate (AQDS). *Journal of Environmental Sciences, 38*, 87–94.

Liu, J., Chen, T., Qi, Z., Yan, J., Buekens, A., & Li, X. (2014). Thermal desorption of PCBs from contaminated soil using nano zerovalent iron. *Environmental Science and Pollution Research International, 21*(22), 12739–12746.

Matheus, D. R., Bononi, V. L. R., & Machado, K. M. G. (2000). Biodegradation of hexachlorobenzene by basidiomycetes in soil contaminated with industrial residues. *World Journal of Microbiology and Biotechnology, 16*(5), 415–421.

Meijer, S. N., Ockenden, W. A., Sweetman, A., Breivik, K., Grimalt, J. O., & Jones, K. C. (2003). Global distribution and budget of PCBs and HCB in background surface soils: Implications for sources and environmental processes. *Environmental Science and Technology, 37*(4), 667–672.

Oonnittan, A., Shrestha, R. A., & Sillanpaa, M. (2008). Remediation of hexachlorobenzene in soil by enhanced electrokinetic Fenton process. *Journal of Environmental Science and Health Part A Toxic/hazardous Substances & Environmental Engineering, 43*(8), 894–900.

Oonnittan, A., Shrestha, R. A., & Sillanpaa, M. (2009). Removal of hexachlorobenzene from soil by electrokinetically enhanced chemical oxidation. *Journal of Hazardous Materials, 162*(2–3), 989–993.

Pan, X., Wei, J., Qu, R., Xu, S., Chen, J., Al-Basher, G., Li, C., Shad, A., Dar, A. A., & Wang, Z. (2020). Alumina-mediated photocatalytic degradation of hexachlorobenzene in aqueous system: Kinetics and mechanism. *Chemosphere, 257*, 127256.

Shih, Y. H., Chen, Y. C., Chen, M. Y., Tai, Y. T., & Tso, C. P. (2009). Dechlorination of hexachlorobenzene by using nanoscale Fe and nanoscale Pd/Fe bimetallic particles. *Colloid Surface A, 332*, 84–89.

Shih, Y. H., Hsu, C. Y., & Su, Y. F. (2011). Reduction of hexachlorobenzene by nanoscalezero-valentiron:Kinetics, pH effect, and degradation mechanism. *Separation and Purification Technology, 76*, 268–274.

Song, Y., Bian, Y., Wang, F., Herzberger, A., Yang, X., Gu, C., & Jiang, X. (2017). Effects of biochar on dechlorination of hexachlorobenzene and the bacterial community in paddy soil. *Chemosphere, 186*, 116–123.

Starek-Swiechowicz, B., Budziszewska, B., & Starek, A. (2017). Hexachlorobenzene as a persistent organic pollutant: Toxicity and molecular mechanism of action. *Pharmacological Reports, 69*(6), 1232–1239.

Su, Y. F., Hsu, C. Y., & Shih, Y. H. (2012). Effects of various ions on the dechlorination kinetics of hexachlorobenzene by nanoscale zero-valent iron. *Chemosphere, 88*(11), 1346–1352.

Takagi, K., Iwasaki, A., Kamei, I., Satsuma, K., Yoshioka, Y., & Harada, N. (2009). Aerobic mineralization of hexachlorobenzene by newly isolated pentachloronitrobenzene-degrading Nocardioides sp. strain PD653. *Applied and Environment Microbiology, 75*(13), 4452–4458.

Umulisa, V., Kalisa, D., Skutlarek, D., & Reichert, B. (2020). First evaluation of DDT (dichlorodiphenyltrichloroethane) residues and other persistence organic pollutants in soils of rwanda: Nyabarongo urban versus rural wetlands. *Ecotoxicology and Environmental Safety, 197*, 110574.

Wan, J., Li, Z., Lu, X., & Yuan, S. (2010). Remediation of a hexachlorobenzene-contaminated soil by surfactant-enhanced electrokinetics coupled with microscale Pd/Fe PRB. *Journal of Hazardous Materials, 184*(1–3), 184–190.

Wang, G., Lu, Y., Han, J., Luo, W., Shi, Y., Wang, T., & Sun, Y. (2010). Hexachlorobenzene sources, levels and human exposure in the environment of China. *Environment International, 36*(1), 122–130.

Wu, Q., Milliken, C. E., Meier, G. P., Watts, J. E., Sowers, K. R., & May, H. D. (2002). Dechlorination of chlorobenzenes by a culture containing bacterium DF-1, a PCB dechlorinating microorganism. *Environmental Science and Technology, 36*(15), 3290–3294.

Yan, D. Z., Mao, L. Q., Li, C. Z., & Liu, J. (2015). Biodegradation of hexachlorobenzene by a constructed microbial consortium. *World Journal of Microbiology & Biotechnology, 31*(2), 371–377.

Yuan, S., Tian, M., & Lu, X. (2006a). Electrokinetic movement of hexachlorobenzene in clayed soils enhanced by Tween 80 and beta-cyclodextrin. *Journal of Hazardous Materials, 137*(2), 1218–1225.

Yuan, S., Tian, M., & Lu, X. (2006b). Microwave remediation of soil contaminated with hexachlorobenzene. *Journal of Hazardous Materials, 137*(2), 878–885.

Yuan, Y., Ning, X. A., Zhang, Y., Lai, X., Li, D., He, Z., & Chen, X. (2020). Chlorobenzene levels, component distribution, and ambient severity in wastewater from five textile dyeing wastewater treatment plants. *Ecotoxicology and Environmental Safety, 193*, 110257.

Zhou, D. Q. (2002). *Text book of microbiology*. Beijing: Higher Education Press.

Zhou, Q., Wang, J., Meng, B., Cheng, J., Lin, G., Chen, J., Zheng, D., & Yu, Y. (2013). Distribution and sources of organochlorine pesticides in agricultural soils from central China. *Ecotoxicology and Environmental Safety, 93*, 163–170.

Zhu, N., Luan, H., Yuan, S., Chen, J., Wu, X., & Wang, L. (2010). Effective dechlorination of HCB by nanoscale Cu/

Fe particles. *Journal of Hazardous Materials, 176*(1–3), 1101–1105.